

## Subcritical dynamo and hysteresis in a Babcock-Leighton type kinematic dynamo model

Vindya Vashishth<sup>1</sup>, Bidya Binay Karak<sup>1</sup> and Leonid Kitchatinov<sup>2,3</sup>

<sup>1</sup> Department of Physics, Indian Institute of Technology (BHU), Varanasi 221005, India

<sup>2</sup> Institute of Solar-Terrestrial Physics SB RAS, Lermontov Str. 126A, 664033, Irkutsk, Russia

<sup>3</sup> Pulkovo Astronomical Observatory, Pulkovskoe Sh.65, St. Petersburg, 196140, Russia;  
[vindyavashishth.rs.phy19@itbhu.ac.in](mailto:vindyavashishth.rs.phy19@itbhu.ac.in)

Received 2021 May 27; accepted 2021 July 17

**Abstract** In the Sun and Sun-like stars, it is believed that cycles of the large-scale magnetic field are produced due to the existence of differential rotation and helicity in the plasma flows in their convection zones (CZs). Hence, it is expected that for each star, there is a critical dynamo number for the operation of a large-scale dynamo. As a star slows down, it is expected that the large-scale dynamo ceases to operate above a critical rotation period. In our study, we explore the possibility of the operation of the dynamo in the subcritical region using the Babcock–Leighton type kinematic dynamo model. In some parameter regimes, we find that the dynamo shows hysteresis behavior, i.e., two dynamo solutions are possible depending on the initial parameters—decaying solution if starting with weak field and strong oscillatory solution (subcritical dynamo) when starting with a strong field. However, under large fluctuations in the dynamo parameter, the subcritical dynamo mode is unstable in some parameter regimes. Therefore, our study supports the possible existence of subcritical dynamo in some stars which was previously demonstrated in a mean-field dynamo model with distributed  $\alpha$  and MHD turbulent dynamo simulations.

**Key words:** magnetic field — Sun: activity — Sun: magnetic fields — stars: rotation — stars: dynamo — stars

### 1 INTRODUCTION

It is believed that the convective flows of ionized plasma in the convection zones (CZs) of the Sun and Sun-like stars are responsible for generation of the magnetic field and cycles through the hydromagnetic dynamo (Moffatt 1978; Charbonneau 2020). In this dynamo, differential rotation and helical convective flow play important roles. This is because the differential rotation of the star generates the toroidal field from the poloidal one through the so-called  $\omega$  effect. On the other hand, the helical turbulence induces the poloidal field from the toroidal one which is popularly known as the  $\alpha$  effect. In this type of  $\alpha$ - $\omega$  dynamo model, the governing parameter is the dynamo number, which is defined as,

$$D = \frac{\alpha \Delta \Omega R^3}{\eta^2}, \quad (1)$$

where  $\alpha$  is the measure of  $\alpha$ -effect,  $\Delta \Omega$  is the variation in the angular velocity of the Sun/star,  $R$  is its radius and  $\eta$  is the turbulent magnetic diffusivity (Krause & Rädler 1980). There is a critical dynamo number ( $D_c$ ) below which

the dynamo is not possible and the initial magnetic field decays. The regime below  $D_c$  is known as the subcritical regime and that above  $D_c$  is called the supercritical regime (Choudhuri 1998; Kumar et al. 2021).

Since the rotation rate of a star decreases with age (Skumanich 1972; Rengarajan 1984), the dynamo number  $D$  is expected to decrease as the star spins down (Kitchatinov & Nepomnyashchikh 2017). Therefore, the question is: will the dynamo cease immediately when  $D < D_c$ ? Interestingly, it has been found that the dynamo is still possible when  $D < D_c$ . Kitchatinov & Olemskoy (2010) have described this subcritical dynamo in a kinematic mean-field dynamo model with nonlinear quenching in  $\alpha$  and  $\eta$ . They found that in the subcritical regime, if the dynamo is started with a strong magnetic field, a strong oscillating solution is possible. In contrast, when the dynamo is initiated with a weak field, a decaying solution is produced. Thus this dependence of the magnetic field with the dynamo number exhibits a hysteresis behavior. Further, in a simplified model, Kitchatinov & Nepomnyashchikh (2015) demonstrated that transitions

between two modes (subcritical dynamo with finite magnetic field and supercritical dynamo) qualitatively reproduce two distinct modes in the distribution of solar activity as inferred from cosmogenic isotope content in natural archives (Usoskin et al. 2014). This behavior was further supported by Karak et al. (2015) in the turbulent dynamo simulations.

In the above-mentioned study (Kitchatinov & Olemsky 2010), a helical  $\alpha$ , distributed over the whole CZ, was used. However, recently, there are observational supports for the predominance of the Babcock–Leighton process for the generation of a poloidal field in the Sun (Dasi-Espuig et al. 2010; Kitchatinov & Olemsky 2011; Muñoz-Jaramillo et al. 2013; Priyal et al. 2014; Cameron & Schüssler 2015). Various surface flux transport (Wang et al. 1989; Baumann et al. 2004; Jiang et al. 2014b) and dynamo models (Karak et al. 2014a; Choudhuri 2018; Charbonneau 2020) based on this Babcock–Leighton process alone have been successful in modeling various aspects of solar magnetic fields and cycles. Therefore, in this study, we shall explore the subcritical dynamo in a Babcock–Leighton type solar dynamo model.

As our model is kinematic, we do not capture any nonlinearity in the mean flows. We however consider magnetic field dependence nonlinearity in turbulent diffusivity and Babcock–Leighton  $\alpha$ . While diffusivity quenching is obvious and we have some estimates based on certain approximations (Kitchatinov et al. 1994b; Karak et al. 2014b), the quenching in Babcock–Leighton  $\alpha$  is less constrained. In the Babcock–Leighton process, a poloidal field is produced by the decay and the dispersal of tilted bipolar magnetic regions (BMRs). This tilt has some magnetic field dependence, although its exact dependence is not well constrained (Dasi-Espuig et al. 2010; Jha et al. 2020). There is also a latitudinal variation of BMRs with the solar cycle (Mandal et al. 2017) which may be a source of nonlinear quenching (Jiang 2020; Karak 2020). In our study, we shall consider magnetic field dependent quenching in both diffusivity and  $\alpha$  based on quasi-linear approximation as presented in Ruediger & Kichatinov (1993); Kitchatinov et al. (1994b).

In the Babcock–Leighton  $\alpha$ , there is some inherent randomness as primarily seen in the tilts of BMRs around Joy’s law (Dasi-Espuig et al. 2010; Stenflo & Kosovichev 2012; McClintock et al. 2014; Wang et al. 2015; Arlt et al. 2016; Jha et al. 2020). These fluctuations can have a serious impact on the magnetic cycle and particularly on the existence of the subcritical dynamo branch. Therefore we shall also include fluctuations in the Babcock–Leighton  $\alpha$  term of our dynamo model and check the dynamo behavior in different regimes.

## 2 MODEL

For our study, we consider the magnetic field to be axisymmetric and thus we express it in the following form

$$\mathbf{B}_{\text{total}} = \mathbf{B}_{\mathbf{p}} + \mathbf{B}_{\phi} = \nabla \times [A(r, \theta, t)\hat{\phi}] + B(r, \theta, t)\hat{\phi}, \quad (2)$$

where  $\mathbf{B}_{\mathbf{p}} = \nabla \times [A\hat{\phi}]$  is the poloidal component of the magnetic field and  $B$  is the toroidal component. The evolutions of the poloidal and toroidal fields take the following forms.

$$\frac{\partial A}{\partial t} + \frac{1}{s}(\mathbf{v}_{\mathbf{p}} \cdot \nabla)(sA) = \eta_T \left( \nabla^2 - \frac{1}{s^2} \right) A + S(r, \theta; B), \quad (3)$$

$$\begin{aligned} \frac{\partial B}{\partial t} + \frac{1}{r} \left[ \frac{\partial}{\partial r}(rv_r B) + \frac{\partial}{\partial \theta}(v_{\theta} B) \right] &= \eta_T \left( \nabla^2 - \frac{1}{s^2} \right) B \\ &+ s(\mathbf{B}_{\mathbf{p}} \cdot \nabla)\Omega + \frac{1}{r} \frac{d\eta}{dr} \frac{\partial(rB)}{\partial r}, \end{aligned} \quad (4)$$

where  $s = r \sin \theta$ ,  $\mathbf{v}_{\mathbf{p}} = v_r \hat{\mathbf{r}} + v_{\theta} \hat{\boldsymbol{\theta}}$  is the meridional flow, which is obtained through an observationally-guided analytic formula as given in Karak & Cameron (2016), and  $S$  is the source for the poloidal field. In the classical  $\alpha\Omega$  mean-field model,  $S$  is due to the helical nature of the convective flow. However, in the case of Babcock–Leighton process, the poloidal field is generated near the surface through the decay and dispersal of tilted BMRs. In our axisymmetric model, this process has been routinely parameterized as

$$S(r, \theta; B) = \alpha_{\text{BL}} \bar{B}(\theta, t), \quad (5)$$

where  $\bar{B}(\theta, t)$  is the average toroidal field in a thin layer at the base of the CZ (BCZ) ( $0.675 R_{\odot} < r < 0.725 R_{\odot}$ ) and  $\alpha_{\text{BL}}$  is the parameter for the Babcock–Leighton process. We write,

$$\alpha_{\text{BL}} = \alpha \phi_{\alpha}(\beta), \quad (6)$$

where  $\beta = B/B_0$  with  $B_0$  being the equipartition field strength. The  $\alpha$  is the profile for the usual Babcock–Leighton  $\alpha$  which has the following form

$$\begin{aligned} \alpha &= \frac{\alpha_0}{4} \left[ 1 + \operatorname{erf} \left( \frac{r - 0.95 R_{\odot}}{0.05 R_{\odot}} \right) \right] \\ &\times \left[ 1 - \operatorname{erf} \left( \frac{r - R_{\odot}}{0.01 R_{\odot}} \right) \right] \frac{\sin \theta \cos \theta}{1 + \exp(K)}, \end{aligned} \quad (7)$$

for  $\theta < \pi/2$ ,  $K = 30(\pi/4 - \theta)$  and for  $\theta > \pi/2$ ,  $K = 30(\theta - 3\pi/4)$ .

The  $\phi_{\alpha}(\beta)$  in Equation (6) has the following magnetic field dependent quenching based on quasi-linear approximation as presented in Ruediger & Kichatinov (1993).

$$\phi_{\alpha}(\beta) = \frac{15}{32\beta^4} \left[ 1 - \frac{4\beta^2}{3(1+\beta^2)^2} - \frac{1-\beta^2}{\beta} \arctan \beta \right]. \quad (8)$$

The turbulent diffusivity  $\eta_T$  has the following form

$$\eta_T = \eta\phi_\eta(\beta), \quad (9)$$

where

$$\eta = \eta_0 \left[ \eta_{in} + \left( \frac{1 - \eta_{in}}{2} \right) \left( 1 + \operatorname{erf} \left( \frac{r - x_n}{h_n} \right) \right) \right] \quad (10)$$

with  $\eta_{in} = 10^{-4}$ ,  $x_n = 0.70 R_\odot$ ,  $h_n = 0.05 R_\odot$  and  $\eta_0 = 5 \times 10^{12} \text{ cm}^2 \text{ s}^{-1}$ . We consider a magnetic field dependent quenching in the diffusivity following Kitchatinov et al. (1994a)

$$\phi_\eta(\beta) = \frac{3}{8\beta^2} \left[ 1 + \frac{4 + 8\beta^2}{(1 + \beta^2)^2} + \frac{\beta^2 - 5}{\beta} \arctan \beta \right]. \quad (11)$$

We note that both  $\alpha$  and  $\eta_T$  are quenched through the local magnetic field. In Section 3.2, however, we shall change this prescription and relate  $\alpha$  and  $\eta_T$  through the magnetic field at the BCZ.

The differential rotation  $\Omega$  and the boundary conditions are the same as those used in Nandy & Choudhuri (2002); Chatterjee et al. (2004).

### 3 RESULTS

#### 3.1 Quenching with the Local Field

By including the magnetic field dependent quenching in  $\eta_T$  and  $\alpha$  and by specifying the large-scale flows, such as differential rotation and meridional circulation, we solve the dynamo Equations (3) and (4). We first identify the dynamo transition. To do so, we perform simulations at different values of  $\alpha_0$ , i.e., at different values of dynamo number, defined here as  $D = \alpha_0 \Omega_0 R^3 / \eta_0^2$  (where  $\Omega_0 = 2\pi/T$ ;  $T = 25.38 \text{ d}$ ). We find that when we start the simulations with a very weak magnetic field, the initial magnetic field grows as long as  $\alpha_0 \geq 28.10 \text{ m s}^{-1}$ . The dynamo number corresponds to this  $\alpha_0$ , i.e., the critical dynamo number,  $D_c = 1.086 \times 10^5$ . The blue circular points connecting the dotted line in Figure 1 show  $B_{\text{avg}}$  versus  $\alpha_0$  and  $D$ .  $B_{\text{avg}}$  is computed at  $0.7 R_\odot$  and  $-13^\circ$  latitude and averaged over a few steady cycles. Now, instead of starting the simulation with a weak magnetic field, we start it with the output of an oscillatory solution of a strong magnetic field. We take the output of the simulation performed at  $\alpha_0 = 28.10 \text{ m s}^{-1}$  and execute a new simulation at  $\alpha_0 = 27 \text{ m s}^{-1}$  and then we take the output of this simulation and feed it into a new simulation at a lower  $\alpha_0$ . In this way, we perform several simulations at a progressively lower  $\alpha_0$  by taking the output of the previous simulation at higher  $\alpha_0$ . The orange diamond points connecting the dotted line in Figure 1 shows  $B_{\text{avg}}$  for these simulations. The interesting behavior we observe is that the solutions are different than the ones performed at the same parameters

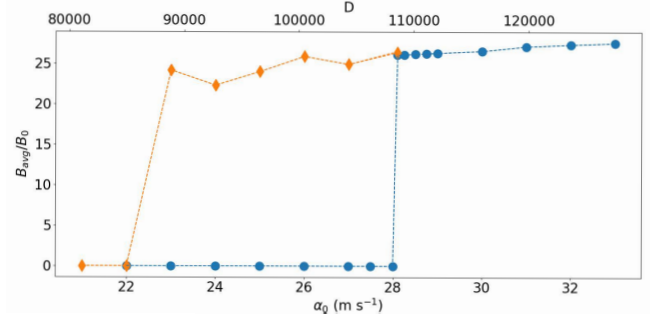


**Fig. 1** Dynamo hysteresis: Variation of the temporal average of the mean toroidal field normalized to  $B_0$  and computed at the BCZ at latitude  $-14^\circ$  ( $B_{\text{avg}}$ ) as a function of  $\alpha_0$  (in  $\text{m s}^{-1}$ ) from simulations starting with a weak field (filled circles) and from simulations starting with strong field of previous simulation (orange diamonds). The corresponding  $D$  is displayed on the top horizontal axis.

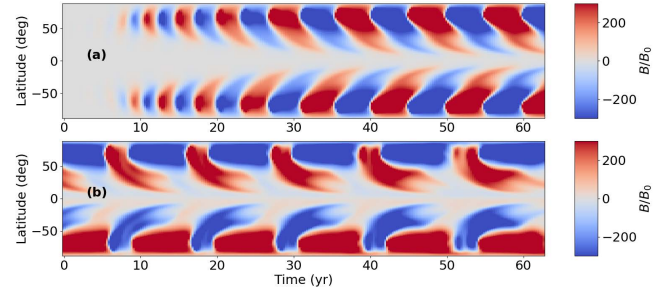


**Fig. 2** (a) Time-latitude distribution of the toroidal field at BCZ from a dynamo simulation at critical dynamo case ( $\alpha = 28.10 \text{ m s}^{-1}$ ) for which the simulation started with a weak field. (b) Same as (a) but from a subcritical dynamo case ( $\alpha = 23 \text{ m s}^{-1}$ ) and the simulation started with a strong field.

but starting with a weak field. We find a wide region in the dynamo parameter space, as displayed in Figure 1, over which the dynamo is decaying when starting with the weak field but produces a strong oscillatory field when starting with a strong field. Overall the dynamo exhibits a hysteresis behavior. This behavior and the subcritical dynamo, for the first time, were discovered in a simple mean-field dynamo with distributed  $\alpha$  (Kitchatinov & Olemskoy 2010). Later dynamo hysteresis was confirmed in magnetohydrodynamics (MHD) simulations of the helical turbulent dynamo with imposed shear (Karak et al. 2015). Recently this was also seen in numerical simulations of turbulent  $\alpha^2$  dynamo (Oliveira et al. 2021).

As discussed in Kitchatinov & Olemskoy (2010), the imposed magnetic-field dependent nonlinearity in turbulent diffusivity and  $\alpha$  make the behavior of the effective dynamo number  $D_{\text{eff}} = \alpha_0 \phi_\alpha(\beta) \Omega R^3 / \eta_0^2 \phi_\eta(\beta)^2$  non-monotonic. When the magnetic field is large ( $\beta \gg 1$ ),  $D_{\text{eff}}$  decreases with the increase of  $\beta$  ( $D_{\text{eff}} \sim \beta^{-1}$ ). In contrast, when  $\beta$  is small ( $\beta \ll 1$ ),  $D_{\text{eff}}$  increases

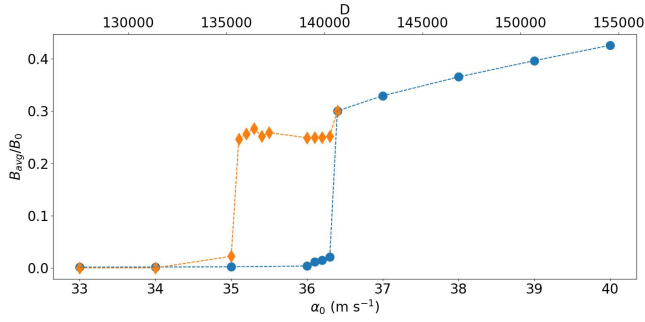


**Fig. 3** Same as Fig. 1 but obtained from simulations in which  $\alpha_{\text{BL}}$  and  $\eta_{\text{T}}$  are related to the toroidal field at the BCZ.

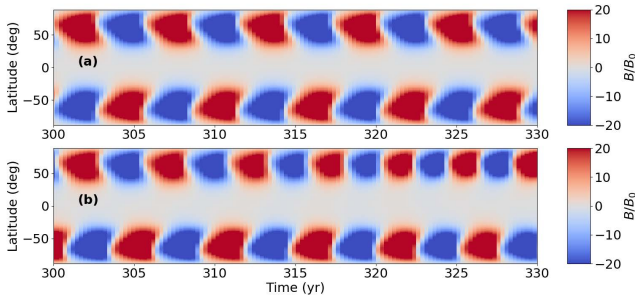


**Fig. 4** Butterfly diagrams for (a) toroidal field at BCZ for critical dynamo for the case ( $\alpha_0 = 36.40 \text{ m s}^{-1}$ ) when the simulation started with a weak magnetic field and (b) for subcritical dynamo case ( $\alpha_0 = 35 \text{ m s}^{-1}$ ) and started with the output of a strong oscillatory solution at  $\alpha_0 = 36 \text{ m s}^{-1}$ .

with the increase of  $\beta$  ( $D_{\text{eff}} \sim D(1 + 16\beta^2/7)$ ); see figure 1 of [Kitchatinov & Olemskoy \(2010\)](#). Thus, when the simulation is started with a very weak field,  $D_{\text{eff}}$  remains small and cannot trigger the dynamo. On the other hand, when the simulation is started with a strong field ( $\beta \sim 1$ ),  $D_{\text{eff}}$  becomes large enough to produce dynamo action.

The time-latitude distributions of the toroidal magnetic fields from a simulation at critical  $\alpha_0 = 28.10 \text{ m s}^{-1}$  (starting with a weak field) and from a subcritical case at  $\alpha_0 = 23 \text{ m s}^{-1}$  (starting with a strong initial field) are displayed in Figure 2. We observe regular polarity reversal and some migration towards the equator. The cycle period is much shorter than the solar value. This short cycle is due to our chosen value of  $\eta_0$  ( $= 5 \times 10^{12} \text{ cm}^2 \text{ s}^{-1}$ ). The high diffusivity always tends to produce a short cycle ([Karak & Choudhuri 2012](#); [Karak & Cameron 2016](#)) unless we reduce the diffusivity at BCZ drastically and/or include a strong downward magnetic pumping ([Kitchatinov & Olemskoy 2012](#); [Karak & Cameron 2016](#)). In fact, if we do not include the nonlinearity in diffusivity, then the cycle period is even shorter ( $\sim 0.83 \text{ yr}$ ).

One aspect of all these simulations is that they produce an unexpectedly strong magnetic field near the BCZ. In

Figures 1 and 2 we observe that the magnetic field strength is several tens of times stronger than  $B_0$ . This strong field is caused by the strongly quenched diffusivity near the BCZ. We recall from Equations (6) and (9) that  $\alpha_{\text{BL}}$  and  $\eta_{\text{T}}$  are related to magnetic field locally. Near the BCZ, the magnetic field is usually stronger than that near the surface and thus at the BCZ,  $\eta_{\text{T}}$  is reduced strongly, but  $\alpha_{\text{BL}}$  is zero there. Hence this strongly reduced diffusivity near the BCZ in our Babcock–Leighton type dynamo is causing this strong magnetic field. This strong magnetic field is indeed in agreement with the super-equipartition field which was a prediction of the thin flux-tube simulations ([D’Silva & Choudhuri 1993](#); [Caligari et al. 1995](#)).

## 3.2 Quenching with the Non-local Field

### 3.2.1 Regular dynamo solutions and hysteresis

The Babcock–Leighton  $\alpha$  is a nonlocal process in which the magnetic field at the BCZ acts as the seed for the poloidal field; see Equation (5). Therefore, instead of connecting  $\alpha_{\text{BL}}$  and  $\eta_{\text{T}}$  with the local magnetic field, we now connect them with the magnetic field at the BCZ, i.e.,

$$\alpha_{\text{BL}} = \alpha \phi_{\alpha}(\bar{\beta}), \quad (12)$$

$$\eta_{\text{T}} = \eta \phi_{\eta}(\bar{\beta}), \quad (13)$$

where  $\bar{\beta} = \bar{B}/B_0$ . The quenching functions  $\phi_{\alpha}$  and  $\phi_{\eta}$  will be computed from the same Equations (8) and (11) but based on the average toroidal field at BCZ ( $\bar{B}$ ). No other changes are made in the model.

We perform the simulations at different values of  $\alpha_0$  in the same way as we have done to produce Figure 1. Figure 3 features the results. We immediately notice that the magnetic field strength is reduced, at least by an order of magnitude. We again find a regime in the dynamo parameter where two solutions are possible: a weak decaying field and a strong oscillatory field, depending on the initial condition. Thus, the dynamo hysteresis is a generic feature in the Babcock–Leighton type solar dynamo.

Figure 4 depicts the time-latitude distribution of the toroidal field from simulation at the critical  $\alpha_0 = 36.40 \text{ m s}^{-1}$  (starting with a weak field) and at the subcritical dynamo,  $\alpha_0 = 35 \text{ m s}^{-1}$  (starting with a strong oscillating field). Although we see some general features of the solar magnetic field in this simulation, the cycle period is considerably reduced. The average period of the magnetic field oscillation is about 2.5 yr. This short cycle period is due to different nonlinear quenching in  $\alpha$  and  $\eta$ . Further, the field is strongest near the poles.

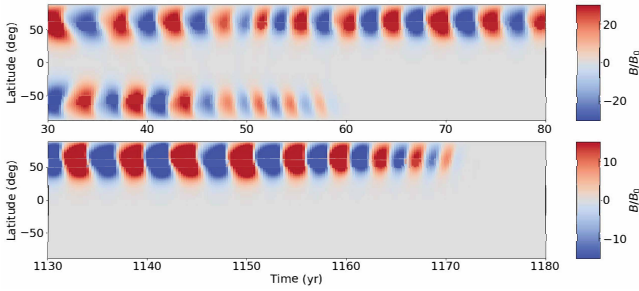


**Fig. 5** Butterfly diagrams of toroidal field for subcritical dynamo at  $\alpha_0 = 35 \text{ m s}^{-1}$  with 20 percent fluctuations. Note that the duration of 80–1130 yr, i.e., the time spans shown in between two panels, is not displayed.

### 3.2.2 Dynamo with fluctuations in $\alpha$

So far in each simulation, all dynamo parameters were kept constant and thus the nonlinearity in our model kept the amplitude of the magnetic cycle nearly equal. However, due to the fluctuating nature of the stellar convection, the dynamo parameter, especially the  $\alpha$ , is subjected to fluctuate around its mean. In the Babcock–Leighton scenario, the fluctuations are primarily seen in the form of scatter in the bipolar active region tilts around Joy’s law (e.g., Stenflo & Kosovichev 2012; Jiang et al. 2014a; McClintock et al. 2014; Wang et al. 2015; Arlt et al. 2016; Jha et al. 2020) and the randomness in flux emergence (Karak & Miesch 2017). On the other hand, in the turbulent mean-field  $\alpha$ , the scatter is unavoidable due to finite numbers of convection cells (Choudhuri 1992). The fluctuations in  $\alpha$  cause the polar field to change and thus make the magnetic cycle unequal as observed in the Sun and Sun-like stars. This has been already incorporated in many studies for modeling the irregular aspects of solar cycles (e.g., Charbonneau & Dikpati 2000; Choudhuri et al. 2007; Choudhuri & Karak 2009; Karak & Choudhuri 2011; Olemskoy & Kitchatinov 2013; Karak et al. 2018).

Motivated by this, we include fluctuations in our Babcock–Leighton  $\alpha$ . To do so, we replace  $\alpha_0$  by  $\alpha_0 = \alpha_0[1 + s(\tau_{\text{corr}}) \times f]$ , where  $s$  is the uniform random number in the interval  $-1 < s < 1$  and  $\tau_{\text{corr}}$  is the coherence time, which is taken as one month—consistent with the mean lifetime of BMRs. Thus, now in our model, the value of  $\alpha_0$  is updated randomly every one month. The level of fluctuations is determined by  $f$ . For example,  $f = 1$  and 0.2 correspond to 100% and 20% fluctuations, respectively.

We find that for subcritical and slightly above critical regimes, this model tends to decay at large fluctuations. The dynamo dies even at 10% fluctuations. Figure 5 depicts the butterfly diagram of a subcritical dynamo ( $\alpha_0 = 35 \text{ m s}^{-1}$ ) in which the magnetic field decayed after about 1000 yr due to large fluctuations. We note that this did not happen simultaneously in two hemispheres. Thus the subcritical branch is unstable under the large

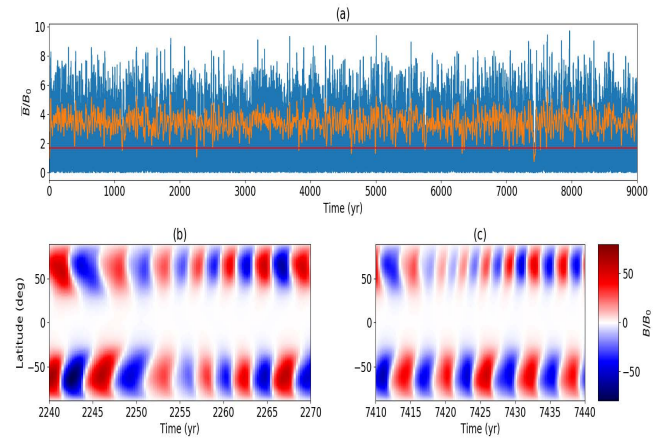


**Fig. 6** (a) Time series plot along with its smoothed curve (yellow) of toroidal magnetic flux. Red horizontal line signifies half of the mean of this smooth curve. (b) and (c) Butterfly diagrams of toroidal field for the two grand minima. These are obtained from a supercritical dynamo at  $\alpha_0 = 40 \text{ m s}^{-1}$ .

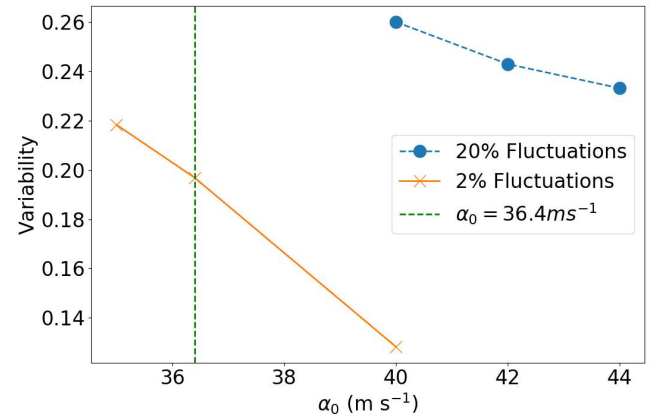


**Fig. 7** Variation of variability with respect to the increase in  $\alpha_0$  with 2% fluctuations (orange solid line) and with 20% fluctuations (blue dashed line).

fluctuations. We have checked that if the fluctuation level is below 10%, then the dynamo does not decay immediately; sometimes it decays in a few years and sometimes it produces cycles for thousands of years before the decay. This is surprising. However, this problem might be solved by adding a distributed  $\alpha_0$  in the CZ which has been a way for recovering the dynamo from a grand minimum (Karak & Choudhuri 2013; Hazra et al. 2014).

However, in the supercritical regime, the dynamo maintains a stable solution even at very large fluctuations. We observe that when we have included 20% fluctuations, subcritical and critical cases die whereas the supercritical case  $\alpha_0 = 40 \text{ m s}^{-1}$  survives. Hence, the critical dynamo number increases with the increase in the level of fluctuations.

The time series of the toroidal magnetic flux  $\overline{B}$  at the BCZ from a simulation for 9000 yr at  $\alpha_0 = 40 \text{ m s}^{-1}$  is displayed in Figure 6(a).  $\overline{B}$  is computed in a small region with  $r = 0.677 R_\odot - 0.726 R_\odot$  and latitudes:  $10^\circ - 45^\circ$ . We can see that the cycles are now variable, occasionally producing significantly strong and weak cycles. To check whether this simulation produces any grand minima or not, we apply the same method as performed in Usoskin et al. (2007) for the Sun. We bin the data for the duration of one cycle period (which is about 2.5 yr in this simulation), filter the data by applying Gleissberg’s low-pass filter 1-2-2-2-1, and finally, count a grand minimum if these smoothed data fall below 50% of their mean for at least two cycle periods, which is 5 yr in our case. In this way, we detect six grand minima. Two such cases are presented in Figure 6(b) and (c). When we increase the supercriticality of the model by increasing  $\alpha_0$ , the number of grand minima decreases. When  $\alpha_0 \geq 42 \text{ m s}^{-1}$  we do not observe any grand minima. This is in somewhat agreement with the stellar observations because only slowly rotating stars produce grand minima (Baliunas et al. 1995) and slowly rotating stars are expected to have a smaller value of  $\alpha_0$ . This is due to the fact that the efficiency of the Babcock–Leighton process depends on the tilt which is rooted in the rotation of the star (D’Silva & Choudhuri 1993).

The amount of variability of the cycle is obviously more when the fluctuation is more; see Figure 7. To compute the variability, we first compute the peaks of the cycles as measured from the toroidal magnetic field time series  $\overline{B}$ . Then the root mean square of the peaks divided by the mean is taken as the variability. The variability decreases with the increase of supercriticality of the model ( $\alpha_0$ ).

#### 4 CONCLUSIONS

In this work, we have applied an axisymmetric kinematic solar dynamo model with a Babcock–Leighton  $\alpha_{\text{BL}}$  as the source of the poloidal field to explore the subcritical dynamo and the hysteresis behavior. We have included magnetic field dependent nonlinearities in the  $\alpha_{\text{BL}}$  and diffusivity  $\eta_T$  based on the quasi-linear approximation (Ruediger & Kitchatinov 1993; Kitchatinov et al. 1994b). We have included these nonlinearities in two ways. First, we connect the  $\alpha_{\text{BL}}$  and  $\eta_T$  with the local toroidal magnetic field and in the second, we connect these with the toroidal field at the BCZ. We find regular polarity reversals and cycles as long as the dynamo number is above a critical value. We find a regime in the dynamo parameter where two solutions are possible: a weak decaying field and a strong oscillatory field, depending on the initial condition. Hence, the dynamo hysteresis, which was predicted in the distributed  $\alpha \Omega$  dynamo (Kitchatinov & Olemskoy 2010) and turbulent dynamo simulations (Karak et al. 2015),

also survives in Babcock–Leighton type dynamos. Thus, our study along with previous studies provides a possible existence of subcritical dynamo for the execution of large-scale magnetic cycles in Sun-like stars.

By including stochastic fluctuations in  $\alpha_{\text{BL}}$ , we check the stability of these subcritical branches. We find that when  $\alpha_{\text{BL}}$  and  $\eta_T$  are connected with the local magnetic field, the subcritical branch maintains stable magnetic cycles. However, in the other case, when the  $\alpha_{\text{BL}}$  and  $\eta_T$  are connected with the magnetic field at the BCZ, the subcritical branch tends to decay with fluctuations. The supercritical branch is always stable and produces some grand minima. The number of grand minima and the variability of the cycle decrease with the increase of supercriticality (as controlled by the strength of  $\alpha_{\text{BL}}$  in our case).

**Acknowledgements** The authors thank Pawan Kumar and the referee for carefully reviewing the manuscript. Financial Support from the Department of Science and Technology (SERB/DST), India through the Ramanujan fellowship (project No. SB/S2/RJN-017/2018) awarded to B.B.K. is acknowledged. B.B.K. also acknowledges the funding provided by the Alexander von Humboldt Foundation. V.V. acknowledges the financial support from the DST through INSPIRE fellowship. L.K. is thankful for the support from the Russian Foundation for Basic Research (Project 19-52-45002\_Ind) and the Ministry of Science and Higher Education of the Russian Federation.

#### References

- Arlt, R., Senthamizh Pavai, V., Schmiel, C., & Spada, F. 2016, *A&A*, 595, A104
- Baliunas, S. L., Donahue, R. A., Soon, W. H., et al. 1995, *ApJ*, 438, 269
- Baumann, I., Schmitt, D., Schüssler, M., & Solanki, S. K. 2004, *A&A*, 426, 1075
- Caligari, P., Moreno-Insertis, F., & Schussler, M. 1995, *ApJ*, 441, 886
- Cameron, R., & Schüssler, M. 2015, *Science*, 347, 1333
- Charbonneau, P. 2020, *Living Reviews in Solar Physics*, 17, 4
- Charbonneau, P., & Dikpati, M. 2000, *ApJ*, 543, 1027
- Chatterjee, P., Nandy, D., & Choudhuri, A. R. 2004, *A&A*, 427, 1019
- Choudhuri, A. R. 1992, *A&A*, 253, 277
- Choudhuri, A. R. 1998, *The Physics of Fluids and Plasmas: an Introduction for Astrophysicists*
- Choudhuri, A. R. 2018, *Journal of Atmospheric and Solar-Terrestrial Physics*, 176, 5
- Choudhuri, A. R., Chatterjee, P., & Jiang, J. 2007, *Physical Review Letters*, 98, 131103
- Choudhuri, A. R., & Karak, B. B. 2009, *RAA (Research in Astronomy and Astrophysics)*, 9, 953

- Dasi-Espuig, M., Solanki, S. K., Krivova, N. A., et al. 2010, *A&A*, 518, A7
- D’Silva, S., & Choudhuri, A. R. 1993, *A&A*, 272, 621
- Hazra, S., Passos, D., & Nandy, D. 2014, *ApJ*, 789, 5
- Jha, B. K., Karak, B. B., Mandal, S., & Banerjee, D. 2020, *ApJL*, 889, L19
- Jiang, J. 2020, *ApJ*, 900, 19
- Jiang, J., Cameron, R. H., & Schüssler, M. 2014a, *ApJ*, 791, 5
- Jiang, J., Hathaway, D. H., Cameron, R. H., et al. 2014b, *Space Sci. Rev.*, 186, 491
- Karak, B. B. 2020, *ApJL*, 901, L35
- Karak, B. B., & Cameron, R. 2016, *ApJ*, 832, 94
- Karak, B. B., & Choudhuri, A. R. 2011, *MNRAS*, 410, 1503
- Karak, B. B., & Choudhuri, A. R. 2012, *Sol. Phys.*, 278, 137
- Karak, B. B., & Choudhuri, A. R. 2013, *RAA (Research in Astronomy and Astrophysics)*, 13, 1339
- Karak, B. B., Jiang, J., Miesch, M. S., et al. 2014a, *Space Sci. Rev.*, 186, 561
- Karak, B. B., Kitchatinov, L. L., & Brandenburg, A. 2015, *ApJ*, 803, 95
- Karak, B. B., Mandal, S., & Banerjee, D. 2018, *ApJ*, 866, 17
- Karak, B. B., & Miesch, M. 2017, *ApJ*, 847, 69
- Karak, B. B., Rheinhardt, M., Brandenburg, A., et al. 2014b, *ApJ*, 795, 16
- Kitchatinov, L. L., & Olemskoy, S. V. 2010, *Astron. Lett.*, 36, 292
- Kitchatinov, L. L., & Olemskoy, S. V. 2011, *Astronomy Letters*, 37, 656
- Kitchatinov, L. L., & Olemskoy, S. V. 2012, *Sol. Phys.*, 276, 3
- Kitchatinov, L. L., Pipin, V. V., & Ruediger, G. 1994a, *Astronomische Nachrichten*, 315, 157
- Kitchatinov, L. L., Rüdiger, G., & Küker, M. 1994b, *A&A*, 292, 125
- Kitchatinov, L., & Nepomnyashchikh, A. 2015, *Astronomy Letters*, 41, 374
- Kitchatinov, L., & Nepomnyashchikh, A. 2017, *MNRAS*, 470, 3124
- Krause, F., & Rädler, K. H. 1980, *Mean-field Magnetohydrodynamics and Dynamo Theory* (Oxford: Pergamon Press)
- Kumar, P., Karak, B. B., & Vashishth, V. 2021, arXiv e-prints, arXiv:2103.11754
- Mandal, S., Karak, B. B., & Banerjee, D. 2017, *ApJ*, 851, 70
- McClintock, B. H., Norton, A. A., & Li, J. 2014, *ApJ*, 797, 130
- Moffatt, H. K. 1978, *Magnetic Field Generation in Electrically Conducting Fluids* (Cambridge: Univ. Press)
- Muñoz-Jaramillo, A., Dasi-Espuig, M., Balmaceda, L. A., & DeLuca, E. E. 2013, *ApJL*, 767, L25
- Nandy, D., & Choudhuri, A. R. 2002, *Science*, 296, 1671
- Olemskoy, S. V., & Kitchatinov, L. L. 2013, *ApJ*, 777, 71
- Oliveira, D. N., Rempel, E. L., Chertovskih, R., & Karak, B. B. 2021, *Journal of Physics: Complexity*, 2, 025012
- Priyal, M., Banerjee, D., Karak, B. B., et al. 2014, *ApJL*, 793, L4
- Rengarajan, T. N. 1984, *ApJL*, 283, L63
- Ruediger, G., & Kichatinov, L. L. 1993, *A&A*, 269, 581
- Skumanich, A. 1972, *ApJ*, 171, 565
- Stenflo, J. O., & Kosovichev, A. G. 2012, *ApJ*, 745, 129
- Usoskin, I. G., Solanki, S. K., & Kovaltsov, G. A. 2007, *A&A*, 471, 301
- Usoskin, I. G., Hulot, G., Gallet, Y., et al. 2014, *A&A*, 562, L10
- Wang, Y.-M., Colaninno, R. C., Baranyi, T., & Li, J. 2015, *ApJ*, 798, 50
- Wang, Y. M., Nash, A. G., & Sheeley, N. R., J. 1989, *Science*, 245, 712